Stretchable scintillator composites for indirect X-ray detectors

J. Oliveira[a, b], V. Correia[a,b], P. Costa[a,c], A. Francesko[a], G. Rocha[b] and S. Lanceros-Mendez[a, c, d*]

[a]Centro/Departamento de Física, Universidade do Minho 4710-057, Braga, Portugal

[b]Algoritmi Research Center, Universidade do Minho, Campus de Azurém, 4800-058 Guimarães, Portugal

[c]BCMaterials, Parque Científico y Tecnológico de Bizkaia, 48160-Derio, Spain

[d]IKERBASQUE, Basque Foundation for Science, 48013, Bilbao, Spain

*Corresponding author: senentxu.lanceros@bcmaterials.net

ABSTRACT: Flexible and stretchable materials are increasingly being investigated for future technological platforms, polymer based materials being the most suitable candidates for those emerging technologies. This work reports on polymer based scintillator composites based on the thermoplastic elastomer Styrene-Ethylene/Butadiene-Styrene (SEBS) and $Gd_2O_3:Eu^{3+}$ scintillator nanoparticles, to form a polymer-based flexible and stretchable material for X-ray indirect detectors. Further, visible light yield under X-ray irradiation was improved by the inclusion of 2,5 diphenyloxazol (PPO) and (1,4-bis (2-(5-phenioxazolil))-benzol (POPOP) within the polymer matrix. Together with high levels of stretchability, with deformations up to 100%, the films exhibit suitable performance with low mechanical hysteresis (less than 1.5 MJ/m^3 for cycles up to 100% of strain) and reproducibly such as a scintillator material for the

conversion of X-ray radiation into visible radiation. The decrease of just ~13% of the X-ray radiation into visible light upon stretching up to 100% is attributed to a reduction of the effective filler concentration and proves the suitability of the developed materials for large area and stretchable X-ray radiation detectors.

KEYWORDS: X-ray; scintillator; stretchable sensor; flexible sensor

1. Introduction

Flexible electronics is an increasingly growing technology as it allows the development of innovative products, opening new application possibilities [1]. One step further in this concept and a new paradigm for electronics is to achieve stretchable materials that are essential to create stretchable organic electronics, sensors and novel devices [2, 3].

In this context, characteristics such as moldable, flexible, printable and stretchable [4] emerge as one of the most relevant technological research fields nowadays, aiming to improve the applicability and integration of electronic systems [4]. Thus, stretchable electronics will allow applications in close contact to the human body and improve installation on curved interfaces [5, 6], among others**.** In the particular case of radiation detectors, stretchability will reduce the inconvenience caused by the rigid panels of conventional detectors and will allow the integration of sensors for medical monitoring and control on three dimensional architectures/configurations [7]. Stretchable radiation detectors will allow applications in the areas of security equipment and in large strain deformation sensors for medical imaging [8, 9].

Indirect X-ray detectors based on scintillators are a key engineering tool on industrial environment as they are widely used in many business and consumer products with ever

increasing frequency in areas such as medicine and security, among others[10-12]. Traditional indirect X-ray detectors are limited by the scintillators critical properties such as efficiency, response time, light yield, surface roughness and for large area applications, low flexibility and cost [13, 14]. Flexible nanocomposites have been prepared for the development of indirect radiation detectors by dispersing scintillating nanoparticles within a polymer matrix [15, 16]. The polymer matrix allows short scintillation time and low manufacturing costs when compared to current available scintillators [11]. These limitations have led to the search for novel materials [17]. Among them, X-ray detectors from polymer-based scintillator composites have sparked large attention due to their scintillation decay time, thermal stability, flexibility, low cost and an easy fabrication in large areas [11, 18].

Thus, in order to develop flexible and stretchable materials able to convert X-ray radiation into visible radiation, with appropriate mechanical properties, showing thermally stability, chemical and radiation resistance and high energy resolution [18], this work reports on a novel composite based on gadolinium oxide doped with europium (Gd_2O_3:Eu^{3+}) and fluorescence molecules 2,5-dipheniloxazol (PPO) and 1,4-bis-(2-(5-phenioxazolil))-benzol (POPOP) able to efficiently convert X-ray radiation into visible light [19, 20], dispersed into a thermoplastic elastomer polymer. Due to their atomic number, wide band gap (~5.2 eV), , high density (~7.4 g cm^{-3}), proper light yield (~2×10^4 photons.M eV^{-1}) and radioluminescence [21], Gd_2O_3:Eu^{3+} nanoparticles were selected as scintillators. Further, the overall visible light output in the X-ray to electrical conversion process was improved by incorporating the fluorescence molecules PPO and POPOP [22].

The polymer matrix was selected from the elastomer styrene-butadiene-styrene (SBS) family, as these materials show a chemical resistance with highly repeatable deformation [23]. However, applications of SBS in the biomedical area is not recommended due to the low biostability, associated to the double bonds of butadiene present in the elastomeric block [24,

25] . The SBS family are thermoplastic elastomers (TPE), shocinw properties of both rubbers and thermoplastics. They have proven suitability for the development of composite materials for strain sensors applications due to their characteristic large deformation, high flexibility and good optical resistance [26, 27]. Form this family of TPE, the co-polymer Styrene-Ethylene/Butylene-Styrene (SEBS) due to their lower butadiene ratio arises as an efficient and stable binder with high biostability, allowing the biomedical application [24]. Besides that, SEBS present an excellent radiation and temperature resistance, good mechanical properties and good optical properties [28, 29].

In this way, the main objective of this work is the development of an innovative generation of flexible and stretchable materials for large area and stretchable indirect X-ray detectors with applicability in areas such as security and healthcare.

2. Experimental Section

2.1. Materials

The thermoplastic elastomer copolymer SEBS, Calprene CH-6120, with a molecular weight of 245.33 g/mol and a ratio of Ethylene-Butylene/Styrene of 68/32 , was supplied by Dynasol. Toluene was obtained from Panreac with a density of 0.86 g/cm^3 at 20 ºC. Gd_2O_3:Eu^{3+} nanoparticles were obtained from Nanograde® and the fluorescence molecules, PPO and POPOP were obtained from Sigma-Aldrich®. Commercial ink scintillator EJ296 was supplied by Eljen Technology. The chemicals were used as provided by the suppliers.

2.2. Sample preparation

Nanocomposite films with an average thickness of ≈50 μm and nanoparticle content between 0.25 to 1.5 wt.% were prepared by solvent casting. First, the desired amount of Gd_2O_3:Eu^{3+} nanoparticles were added to toluene and placed for dispersion in an ultrasound bath for 3h. Then, SEBS was added to the solution and placed, until complete dissolution of the polymer,

in a Teflon™ mechanical stirrer at 150 rpm. The fluorescent molecules were then added at the concentrations of 1wt.% of PPO and 0.01wt.% of POPOP, respectively [30], in some of the samples. The resulting mixture was placed under mechanical stirring, until homogeneous mixing of the components. To conclude, the solution was spread in a clean glass substrate and let dry, for 24 h at room temperature, until complete solvent evaporation.

2.3. Sample characterization and scintillator composite performance evaluation

The composite films with nanoparticle content of 0.50 wt.% were first sputter-coated with gold and subsequently imaged in a NanoSEM - FEI Nova 200 (FEG/SEM) scanning electron microscope (SEM). The SEM images with magnification ×5K and ×50K were recorded in several regions on the top of the film to study the morphology of the nanoparticles and their distribution in the film. Cross-sections images were also obtained, confirming an average thickness of the samples of ≈50 μm and the good distribution of the nanoparticles along the sample thickness. The ImageJ software was used to determine diameter of the particles. The optical transmittance of the samples was measured by Ultraviolet–Visible (UV-VIS) spectroscopy in a range between 200 to 800 nm with a 1 nm step in a UV-2501PC spectrometer. The stress-strain measurements were performed on a mechanical testing machine (Shimadzu model AG-IS) at room temperature, , with a load cell of 50 N, in the tensile mode. Samples were cut with 10 mm x 8 mm and with a thickness of 50 μm (Fischer Dualscope 603-478, digital micrometer). The mechanical measurements were carried out at a velocity of 5 mm/min. Mechanical hysteresis was performed under the same conditions for 10 loading unloading cycles at different deformation up to 100%. The scintillator material converts X-ray radiation into visible light, thus, the performance of the developed stretchable scintillators was evaluated by subjecting the samples to the X-ray radiation produced by a Bruker D8 Discover diffractometer using Cu Kα incident radiation, powered with a voltage of 40 kV and a current ranging from 0 to 40 mA (output power changes from 0 to 1600 W).

The efficiency of the X-ray to visible conversion was evaluated with an electronic measurement system that allows to quantify the emitted visible wavelength radiation, according to the diagram shown in **Scheme 1**, also when the samples are subjected to different deformation levels.

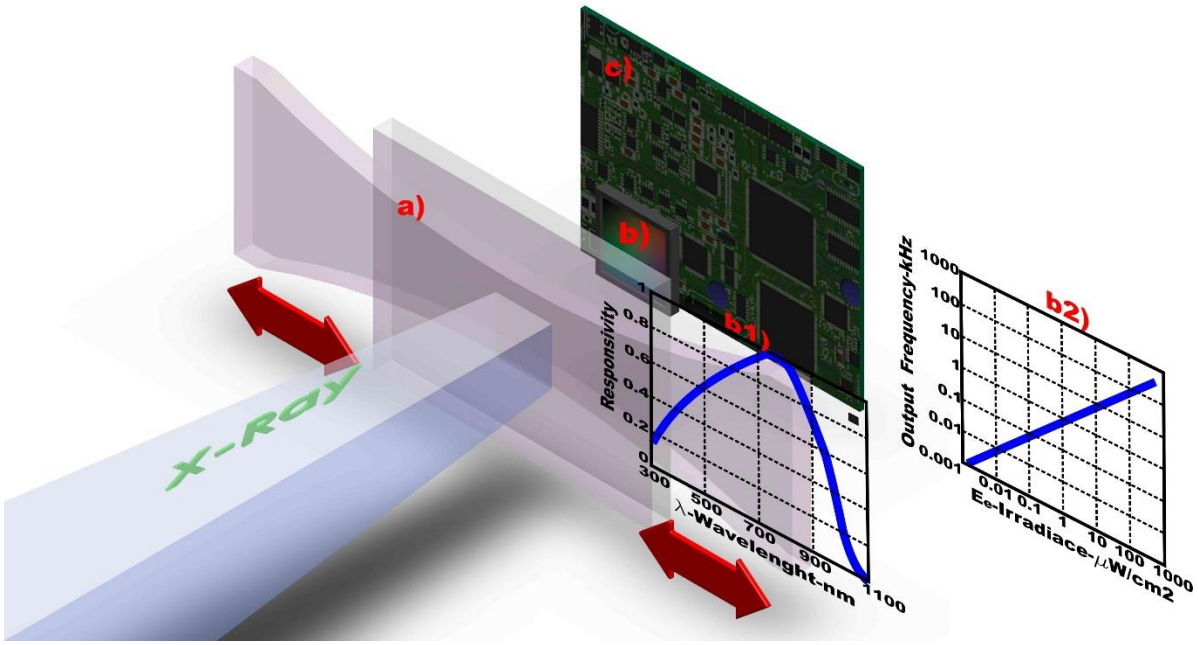

Scheme 1. Diagram of the experimental procedure and the radiation output read-out system for stretchable scintillators samples: a) stretchable scintillators samples, b) light to frequency conversion sensor, b1) converted visible light from the scintillator samples at the corresponding wavelength, b2) sensor (TSL235 from Texas Instruments) output frequency according to irradiated power and c) electronic control system circuit.

The measurements were performed by placing the samples on a home-made support with a mechanical system allowing to apply controlled deformation to the sample (**Scheme 1a**)). This support also contains the light to frequency sensor (**Scheme 1b**), in this case TSL235 from Texas Instruments [31], that convert the radiation in a visible wavelength (**Scheme 1b2**), resulting in a frequency response according to the radiation intensity (**Scheme 1b2**). The

frequency signal response is conditioned and stored over time by an electronic control system circuit (**Scheme 1c**) till the end of the experiment, as the measuring system is placed inside a protection chamber during the irradiation process for securing reasons. The electronic system is composed by a MCU electronic circuit based on the CC1111 from Texas Instruments [31], as it has an on chip Flash memory and is a sub- 1 GhZ RF sytem-on-chip (SoC). Finally, when the experience ends and the X-ray chamber opens, the control system sends the data to a remote platform for analyze by RF. The electronic circuit is powered by a battery, and the voltage is regulated using the switching step-down regulator LM2596 from Texas Instruments, allowing the system to be fully remote. Details on the developed set-up can be found in [22].

3. Results and discussion

Nanocomposite films with an average thickness of ≈50 μm and nanoparticle content between 0.25 to 0.75 wt.% were prepared by solvent casting method and their properties optical, mechanical and performance for X-ray detectors were studied to evaluate the performance as indirect X-ray detectors. The nomenclature SEBS/0.50S-FL is adopted in the manuscript, identifying a SEBS sample with 0.50 wt. % of scintillator nanoparticles and with incorporated fluorescent (FL) molecules.

The morphology and distribution of the nanoparticles within in film were studied by SEM (**Figure 1a and b**). The nanoparticles for small clusters homogeneously distributed in the films (**Figure 1b**), both on the top of the film within the film (cross-section images, not shown). The surface microstructure of the film **Figure 1a** is due to styrene and butadiene rich regions of the SEBS, respectively. SEM images also allow determining that the nanoparticles

are of spherical shape with ~22 nm average diameter (**Figure 1b**). The particles mostly grouped small clusters [32], evenly distributed in the film.

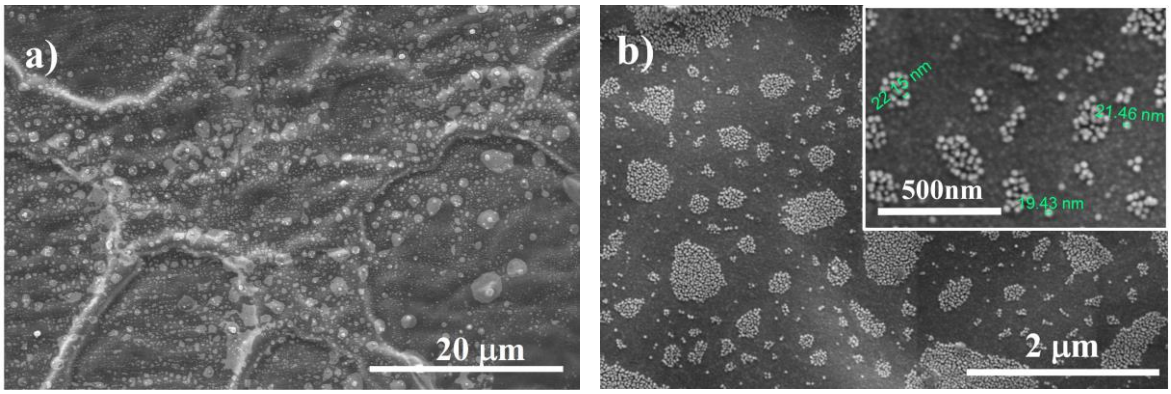

Figure 1. Representative SEM images of the nanocomposite films taken with magnifications of x5K (a) and x50K (b).

The optical properties of the scintillators composites were evaluated and the results are presented in **Figure 2a**. Figure 1a shows that the optical transmittance of the samples as a function of wavelength decrease with increasing scintillator filler content, as increasing filler concentration leads to light dispersion and decreased optical transparency of the films.

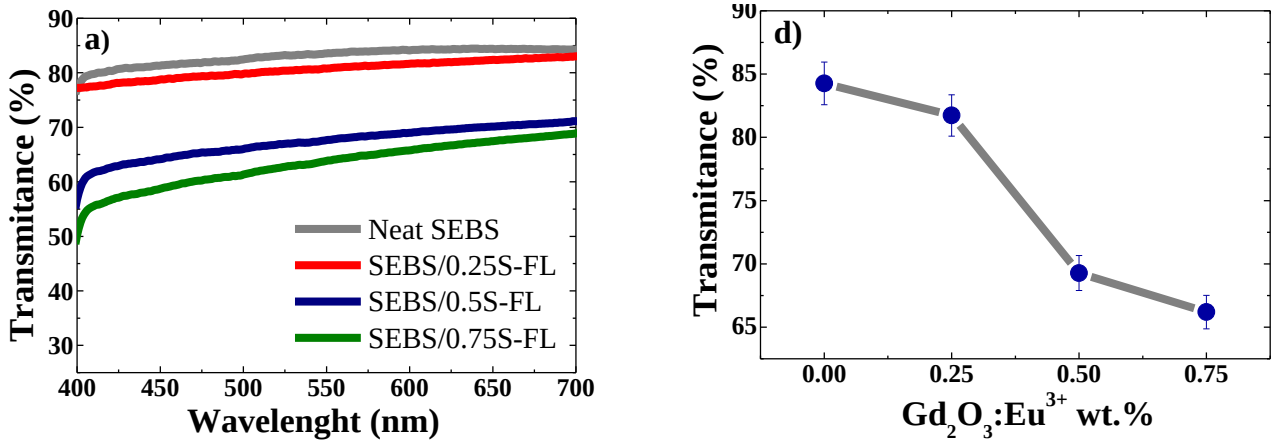

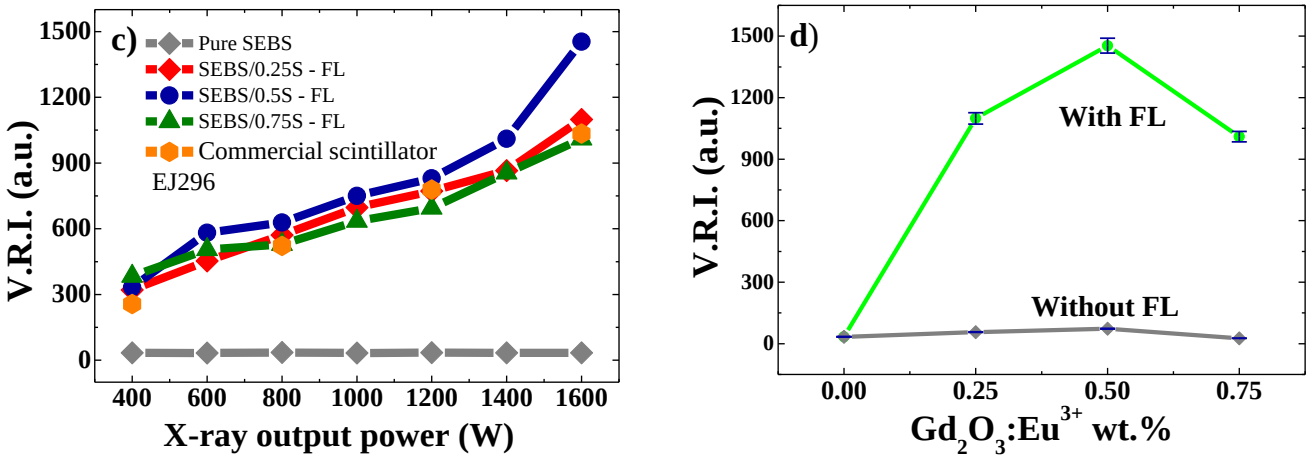

Figure 2. a) Composites optical transmittance as a function of wavelength; b) Composites optical transmittance as a function of $Gd_2O_3:Eu^{3+}$ content, at 611 nm; c) Visible radiation intensity (V.R.I) variation as a function of the X-ray outputpower (W); d) Variation of the visible radiation intensity as a function of $Gd_2O_3:Eu^{3+}$ content (wt %), with and without fluorescence molecules, for a X-ray radiation power of 1600 W;

The main emission peak of the $Gd_2O_3:Eu^{3+}$ is observed at ≈ 611 nm and is related to the red emission transition of Eu^{3+} under X-ray radiation [15, 22]. **Figure 2b** shows the optical transmittance as a function of $Gd_2O_3:Eu^{3+}$ content, at a wavelength of 611nm. The transmittance at ≈ 611 nm suffers a decrease with increasing of scintillator nanoparticle content due to increased light dispersion [22] which leads to the decrease of the composites transmittance from 85% for the pristine polymer to around 65% for the higher filler concentrations.

X-ray radiation was projected into the $Gd_2O_3:Eu^{3+}$/PPO/POPOP/SEBS composite and the conversion into visible light was measured, in order to test and prove the good performance of the composites for the development of X-ray indirect radiation detectors. **Figure 2c** shows the variation of the visible radiation intensity (V.R.I.) as a function of the X-ray intensity. The intensity of the converted visible radiation increases with increasing X-ray output power. It is shown that higher X-ray power and higher scintillators nanoparticle content leads to a higher

number of produced visible photons [18]. The VRI of the composite was compared with the VRI of a commercial ink scintillator, EJ296. This scintillator was chosen as it is based on polyvinyltoluene, has a density of 1.02 $g.cm^{-3}$ and a scintillation efficiency of 9000 photons/MeV^{-1}. As it can be seen, the composite with 0.5 wt.% of Gd2O3:Eu3+ presents a better performance compared with the commercial scintillator, showing also the advantage for applications where stretchability can be taken to advantage, as it will be shown later. The variation of V.R.I. as a function of scintillator nanoparticles content is shown in **Figure 2d**.

Figure 2d shows that the fluorescence molecules inclusion on the scintillation process also improves composite scintillation performance: the introduction of small amounts of fluorescence molecules and scintillator nanoparticles confirms to be the better approach for improving the performance of polymer-based composites for X-ray indirect detector applications, through the mechanism schematically represented in **Figure 2a**.

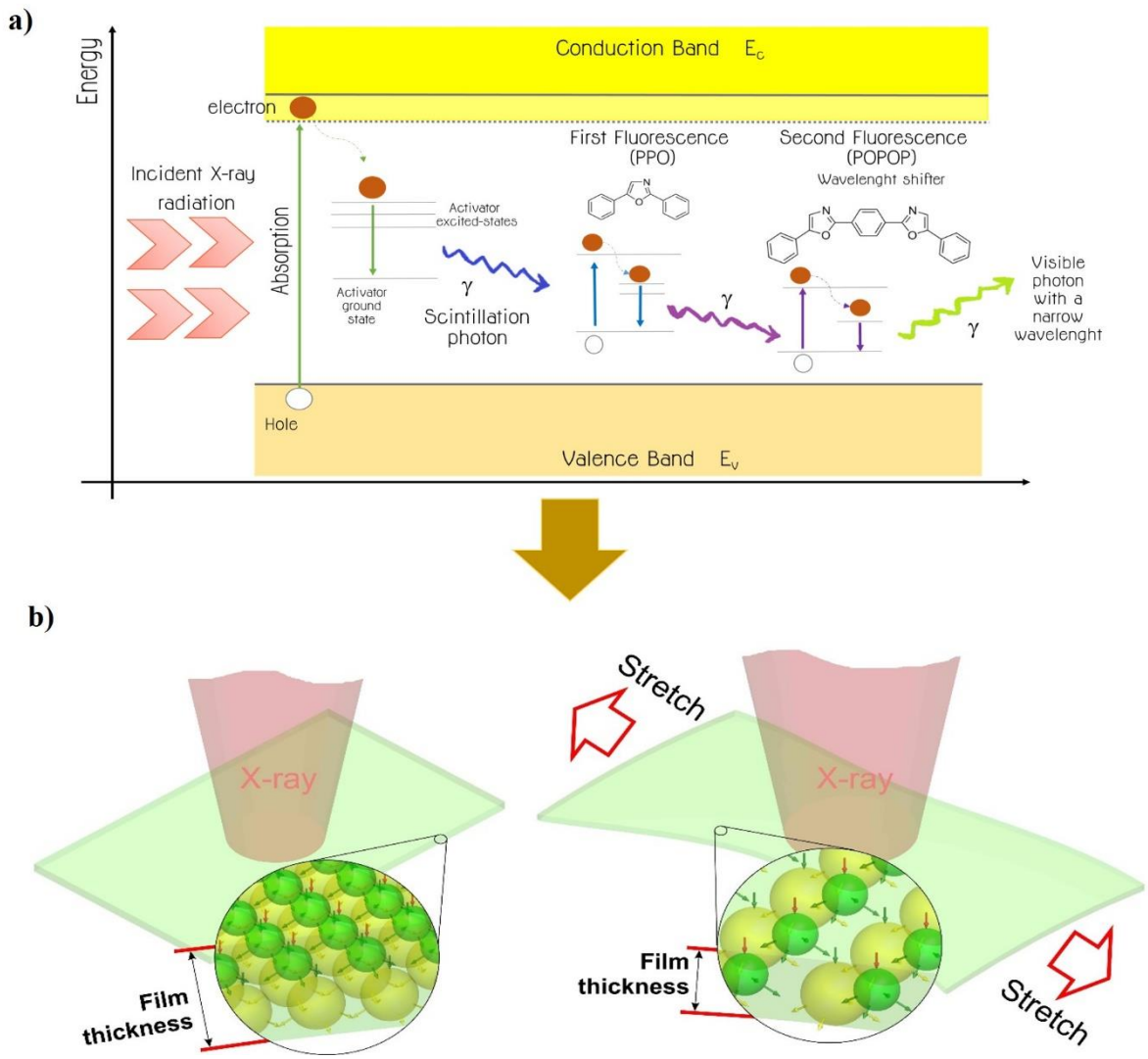

Figure 3. a) Schematic representation of the main physical processed within the scintillator composite. b) Schematic representation of the distribution of the scintillators nanoparticles and fluorescence molecules upon stretching.

Figure 3a shows the scintillator process that occurs on the activated crystals. The interaction between the X-ray radiation and the scintillators nanoparticles generates a deep hole and a hot electron. A sequence of relaxation process including multiplication and thermalization migration lead to a huge number of relaxed electron-hole which must be transferred to the light emitting species (In order to simplify the scintillation process understanding, the recombination of holes and the interactions that will occurs on polymer are not represented in

Figure 3a). Then, the electrons migrate to the activator excited state and the holes in the valence band migrate to the activator ground state [33]. The transition of electrons from an activated center excited-state orbital to an activation center ground-state leads to a production of a scintillation photon [33]. The fluorescence molecules (FL) absorbs this scintillation energy that re-emits at larger wavelength, in the visible wavelength range [24]. PPO absorbs and re-emits the radiation transfer and that will increase the light yield and the POPOP additionally works as a wavelength shifter [34, 35] which will re-emit the photon that will be detected by the photodetector [36]. This process allows the conversion of the shorter emission wavelength scintillators nanoparticles at 611nm to a longer wavelength light correspondent to the maximum photodetector spectral responsivity (The sensor responds over the light range of 300nm to 1100nm showing a maximum spectral response at around 800nm) [31].

It can be seen that the visible radiation yield strongly increases with Gd_2O_3:Eu^{3+} nanoparticle content as well as with the introduction of scintillators nanoparticles and fluorescence molecules up to 0.50 wt%, decreasing for higher concentrations. The detected increase is a consequence of a significant contribution of the scintillator nanoparticles to the increase of the composite density which enhances the x-ray absorption. The decrease for higher particle concentration is a consequence of the decreased optical transparency of the composite, as it can be observed in **Figure 2a**.

Finally, the suitability of the developed composites for flexible and stretchable indirect X-ray indirect detector applications was estimated. The composite with 0.50 wt.% content of Gd_2O_3:Eu^{3+} was chosen as it shows the best performance for the X-ray radiation conversion into visible radiation.

Figure 4a shows the intensity of the converted visible radiation light at an X-ray power of 1600W as a function of the applied strain up to 100%.

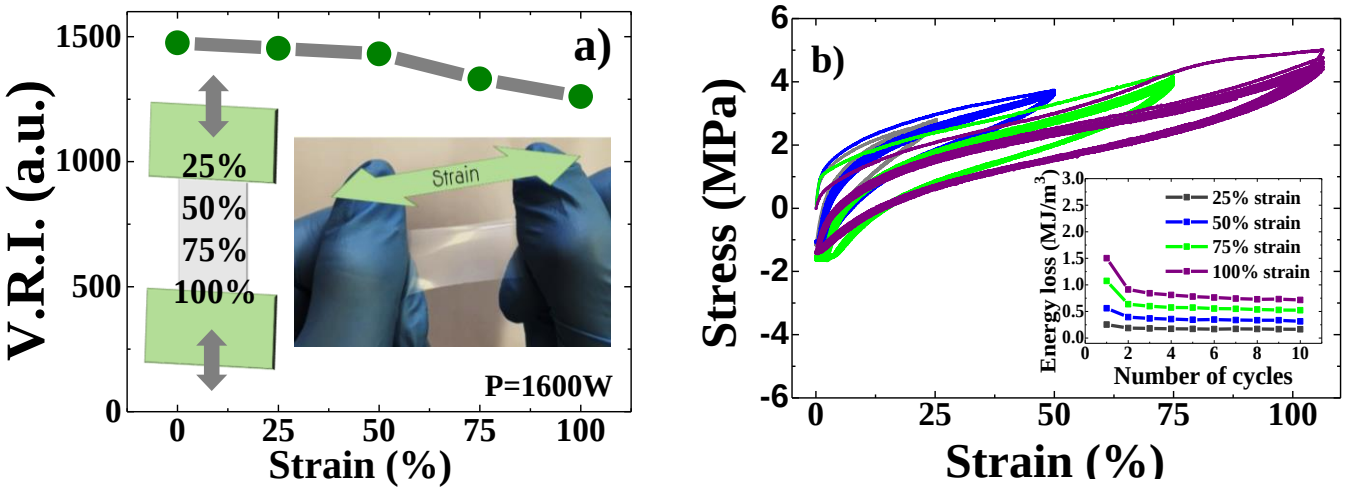

Figure 4. a) of the Visible radiation intensity variation as a function of applied strain on the SEBS/0.5S-FL composite at an X-ray power output of 1600W; b) strain recovery curves with the respective strain of 25, 50, 75 and 100% for the SEBS/0.5S-FL composite and (inset) energy losses for the composites as a function of mechanical strain (between 25% to 100% of strain), for 10 load–unload cycles.

It is observed that increasing applied strain up to 100% leads just to a small decrease of ~13% in the visible radiation intensity output, the scintillator material remaining fully functional. This effect is related to the reduction of the effective distribution of filler concentration, as the thickness decreases, leading to higher optimal transmittance: film stretching leads to a decrease of the film thickness, reducing thus the amount of material in the x-ray beam**. Figure 3b** shows the schematic representation of the microscopic variation of the nanoparticle distribution upon stretching: polymer stretching leads to redistribution of the fillers, having as a result a decrease in the visible radiation conversion efficiency due to a decrease of the filler content by unit area.

The reproducibility of mechanical behavior was measured by the stress-strain curves up to 100% strain, as represented in Figure 4b for the SEBS/0.5S-FL composite. The composite shows excellent elasticity and reproducibility over cycling tests, with a mechanical hysteresis

that increases with increasing applied strain. The inset of Figure 4b shows the mechanical energy dissipate during 10 load-unload cycles for 25, 50, 75 and 100% of applied strain, showing that the mechanical hysteresis leads to a stabilization after the firsts 2 or 3 cycle for the different applied strains.

Thus, this work shows the suitability of the SEBS/0.5S-FL composites for the development of large deformation indirect X-ray detectors.

4. Conclusions

Polymer-based scintillators materials have been developed based on thermoplastic elastomer SEBS composites with a combination of $Gd_2O_3:Eu^{3+}$ scintillator nanoparticles and fluorescence molecules, 2,5diphenyloxazol (PPO) and (1,4-bis (2,5-phenioxazolil))-benzol (POPOP), in order to enhance the visible light output.

This work demonstrated a new type of flexible and stretchable composite material for indirect X-ray detectors with simple, fast and low cost fabrication.

The SEBS/0.5-FL composites presents suitable optical properties in the visible spectral range with an optical transmittance of ~70% at 611nm. Further, the composite maintains excellent elasticity after applied strains of 100% and the stretchability of the scintillator composites does not significantly affects the performance of the X-ray radiation into visible light conversion, proving to be an efficient material for the development of large area stretchable and flexible polymer based X-ray detectors.

Further, these composites also arise as suitable and novel materials for emerging applications in the area of stretchable electronics.

ACKNOWLEDGEMENT

The authors thank FEDER funds through the COMPETE 2020 Programme and National Funds through FCT - Portuguese Foundation for Science and Technology under Strategic Funding UID/FIS/04650/2013 and projects PTDC/EEI-SII/5582/2014 and PTDC/CTM-ENE/5387/2014. J.O., P. C., V. C. and A.F. also thank the FCT for the SFRH/BPD/98219/2013, SFRH/BPD/110914/2015, SFRH/BPD/97739/2013 and SFRH/BPD/104204/2014 grants, respectively. The authors acknowledge funding the Basque Government Industry Department under the ELKARTEK program. Thanks to Dynasol (Spain) for kindly supplying the thermoplastic elastomers.

REFERENCES

[1] Segev-Bar M, Haick H. Flexible sensors based on nanoparticles. ACS Nano. 2013;7:8366-78.
[2] Park J, You I, Shin S, Jeong U. Material approaches to stretchable strain sensors. ChemPhysChem. 2015;16:1155-63.
[3] Knoll GF. Radiation Detection and Measurement: Wiley; 2000.
[4] Wu Z, Hjort K, Jeong SH. Microfluidic stretchable radio-frequency devices. Proceedings of the IEEE. 2015;103:1211-25.
[5] Yoon S, H. K, S. Chang. Highly Stretchable and Transparent Microfluidic Strain Sensors for Monitoring Human Body Motions. ACS Applied Materials & Interfaces. 2015;7:27562-70.
[6] Reuss RH. Macroelectronics: Perspectives on Technology and Applications. Proceedings of the IEEE. 2005;93:1239-56.
[7] Löher T, Seckel M, Ostmann A. Electronics System Integration Technology Conference, ESTC 2010 - Proceedings2010.
[8] Kim SJ, Choi K, Lee B, Kim Y, Hong BH. Materials for Flexible, Stretchable Electronics: Graphene and 2D Materials. Annual Review of Materials Research. 2015;45:63-84.
[9] Yao S, Zhu Y. Nanomaterial-Enabled Stretchable Conductors: Strategies, Materials and Devices. Advanced Materials. 2015;27:1480-511.
[10] Milbrath BD, Peurrung AJ, Bliss M, Weber WJ. Radiation detector materials: An overview. Journal of Materials Research2008. p. 2561-81.
[11] Cai W, Chen Q, Cherepy N, Dooraghi A, Kishpaugh D, Chatziioannou A, et al. Synthesis of bulk-size transparent gadolinium oxide-polymer nanocomposites for gamma ray spectroscopy. Journal of Materials Chemistry C. 2013;1:1970-6.
[12] Rocha JG, Goncalves LM, Lanceros-Mendez S. Bi 2Te 3-Sb 2Te 3 on polymeric substrate for X-ray detectors based on the seebeck effect. Microsystem Technologies. 2012;18:1-8.
[13] Nikl M. Scintillation detectors for x-rays. Measurement Science and Technology. 2006;17:R37-R54.

[14] Quaranta A, Carturan SM, Marchi T, Kravchuk VL, Gramegna F, Maggioni G, et al. Optical and scintillation properties of polydimethyl-diphenylsiloxane based organic scintillators. IEEE Transactions on Nuclear Science. 2010;57:891-900.
[15] Cha BK, Lee SJ, Muralidharan P, Kim JY, Kim DK, Lee DH, et al. Synthesis and scintillation properties of nano Gd2O 3(Eu) scintillator for high resolution X-ray imaging applications. Nuclear Instruments and Methods in Physics Research, Section A: Accelerators, Spectrometers, Detectors and Associated Equipment. 2010;619:174-6.
[16] Lujan RA, Street RA. Flexible X-Ray Detector Array Fabricated With Oxide Thin-Film Transistors. IEEE Electron Device Letters. 2012;33:688-90.
[17] Weber MJ. Inorganic scintillators: Today and tomorrow. Journal of Luminescence. 2002;100:35-45.
[18] Martins PM, Martins P, Correia V, Rocha JG, Lanceros-Mendez S. Gd2O3:Eu Nanoparticle-Based Poly(vinylidene fluoride) Composites for Indirect X-ray Detection. Journal of Electronic Materials. 2014;44:129-35.
[19] Milinchuk VK, Bolbit NM, Klinshpont ER, Tupikov VI, Zhdanov GS, Taraban SB, et al. Radiation-induced chemical processes in polystyrene scintillators. Nuclear Instruments and Methods in Physics Research, Section B: Beam Interactions with Materials and Atoms. 1999;151:457-61.
[20] Oliveira J, Martins PM, Martins P, Correia V, Rocha JG, Lanceros-Mendez S. Increasing X-ray to visible transduction performance of Gd2O3:Eu3+PVDF composites by PPO/POPOP addition. Composites Part B: Engineering. 2016;91:610-4.
[21] García-Murillo A, Le Luyer C, Dujardin C, Martin T, Garapon C, Pédrini C, et al. Elaboration and scintillation properties of Eu3+-doped Gd2O3 and Lu2O3 sol-gel films. Nuclear Instruments and Methods in Physics Research, Section A: Accelerators, Spectrometers, Detectors and Associated Equipment. 2002;486:181-5.
[22] Oliveira J, Martins PM, Martins P, Correia V, Rocha JG, Lanceros-Mendez S. Gd2O3:Eu3+/PPO/POPOP/PS composites for digital imaging radiation detectors. Applied Physics A: Materials Science and Processing. 2015;121:581–7.
[23] Allier CP, Hollander RW, Van Eijk CWE, Sarro PM, De Boer M, Czirr JB, et al. Thin photodiodes for a neutron scintillator silicon-well detector. IEEE Transactions on Nuclear Science. 2001;48:1154-7.
[24] Ribeiro S, Costa P, Ribeiro C, Sencadas V, Botelho G, Lanceros-Méndez S. Electrospun styrene-butadiene-styrene elastomer copolymers for tissue engineering applications: Effect of butadiene/styrene ratio, block structure, hydrogenation and carbon nanotube loading on physical properties and cytotoxicity. Composites Part B: Engineering. 2014;67:30-8.
[25] Agarwal S, Wendorff JH, Greiner A. Use of electrospinning technique for biomedical applications. Polymer. 2008;49:5603-21.
[26] Wang ZF, Wang P, Ye XY, Jiang B. IEEE Conference on Nanotechnology. **2009**:756-7.
[27] Hu M, Zhang N, Guo Q, Cai X, Zhou S, Yang J. Soluble salt-driven matrix swelling of a block copolymer for rapid fabrication of a conductive elastomer toward highly stretchable electronics. Materials and Design. 2016;100:263-70.
[28] Ranade SV, Richard RE, Helmus MN. Styrenic block copolymers for biomaterial and drug delivery applications. Acta Biomaterialia. 2005;1:137-44.
[29] Gonçalves BF, Costa P, Oliveira J, Ribeiro S, Correia V, Botelho G, et al. Green solvent approach for printable large deformation thermoplastic elastomer based piezoresistive sensors and their suitability for biomedical applications. Journal of Polymer Science, Part B: Polymer Physics. 2016;54:2092-103.
[30] Ovechkina L, Riley K, Miller S, Bell Z, Nagarkar V. Gadolinium loaded plastic scintillators for high efficiency neutron detection. Physics Procedia. 2009;2:161-70.
[31] Instruments T. May, 2016.
[32] Pires AM, Santos MF, Davolos MR, Stucchi EB. The effect of Eu3+ ion doping concentration in Gd2O3 fine spherical particles. Journal of Alloys and Compounds. 2002;344:276-9.

[33] Derenzo SE, Weber MJ, Bourret-Courchesne E, Klintenberg MK. The quest for the ideal inorganic scintillator. Nuclear Instruments and Methods in Physics Research, Section A: Accelerators, Spectrometers, Detectors and Associated Equipment. 2003;505:111-7.
[34] Liu C, Hajagos TJ, Kishpaugh D, Jin Y, Hu W, Chen Q, et al. Facile Single-Precursor Synthesis and Surface Modification of Hafnium Oxide Nanoparticles for Nanocomposite γ-Ray Scintillators. Advanced Functional Materials. 2015;25:4607-16.
[35] Fernow RC. Introduction to Experimental Particle Physics: Cambridge University Press; 1989.
[36] Quaranta A, Carturan S, Marchi T, Buffa M, Degerlier M, Cinausero M, et al. Doped polysiloxane scintillators for thermal neutrons detection. Journal of Non-Crystalline Solids. 2011;357:1921-5.